Int J CARS
DOI 10.1007/s11548-013-0902-y

ORIGINAL ARTICLE

Fast and robust extraction of surrogate respiratory signal from intra-operative liver ultrasound images

Jiaze Wu · Cheng Li · Su Huang · Feng Liu · Bien Soo Tan · London Lucien Ooi · Haoyong Yu · Jimin Liu

Received: 10 January 2013 / Accepted: 28 May 2013

Abstract
Purpose In model-based respiratory motion estimation for the liver or other abdominal organs, the surrogate respiratory signal is usually obtained by using special tracking devices from skin or diaphragm, and subsequently applied to parameterize a 4D motion model for prediction or compensation. However, due to the intrinsic limits and economical costs of these tracking devices, the identification of the respiratory signal directly from intra-operative ultrasound images is a more attractive alternative.
Methods We propose a fast and robust method to extract the respiratory motion of the liver from an intra-operative 2D ultrasound image sequence. Our method employs a preprocess to remove speckle-like noises in the ultrasound images and utilizes the normalized cross-correlation to measure the image similarity fast. More importantly, we present a novel adaptive search strategy, which makes full use of the inter-frame dependency of the image sequence. This search strategy narrows the search range of the optimal matching, thus greatly reduces the search time, and makes the matching process more robust and accurate.
Results The experimental results on four volunteers demonstrate that our method is able to extract the respiratory signal from an image sequence of 256 image frames in 5 s. The quantitative evaluation using the correlation coefficient reveals that the respiratory motion, extracted near the liver boundaries and vessels, is highly consistent with the reference motion tracked by an EM device.
Conclusions Our method can use 2D ultrasound to track natural landmarks from the liver as surrogate respiratory signal and hence provide a feasible solution to replace special tracking devices.

Keywords Respiratory motion · Ultrasound liver images · Similarity metric · Adaptive searching

J. Wu (✉) · S. Huang · F. Liu · J. Liu
Singapore Bioimaging Consortium, Agency for Science, Technology and Research, #08-01, Matrix, 30 Biopolis Street, Singapore 138671, Singapore
e-mail: wujiaze05@gmail.com; wu_jiaze@sbic.a-star.edu.sg

J. Liu
e-mail: liujm@sbic.a-star.edu.sg

C. Li · H. Yu
Department of Bioengineering, National University of Singapore, Singapore, Singapore

B. S. Tan
Department of Diagnostic Radiology, Singapore General Hospital, Singapore, Singapore

L. L. Ooi
Department of Surgery, Singapore General Hospital, Singapore, Singapore

Introduction

Image-guided robot-assisted surgery and intervention are now used in more and more hospitals to overcome limitations of traditional open and minimally invasive procedures. The most successful and established surgical robot system is the Da Vinci® operating system by Intuitive Surgical Inc. The issues with the Da Vinci system, however, are high cost of system and consumables, long setup time for use, and the absence of built-in intelligence. Despite these issues, it plays an established role in complex surgeries because of the value-added benefits, but its use in simple procedures is conversely limited. To address the use of robots for simple procedures, a new trend [1] in the medical devices is to develop simple image-guided, dedicated, and low-cost robotic systems

Published online: 08 June 2013

for specific surgical and/or interventional procedures. Computational tomography (CT) or magnetic resonance (MR) imaging is able to show higher-resolution details of anatomy structures, but CT imaging has the disadvantage of radiation exposure and potential damage, while MR imaging is expensive and also requires relatively expensive MR-compatible devices; therefore, CT/MR images are usually used in pre-operative planning. On the other hand, ultrasound (US) imaging can provide real-time intra-operative visualization of anatomy structures, but, due to its low contrast, usually costs a lot of time for physicians in target localization and also needs CT or MR imaging for intra- or post-procedure verifications of targeting and ablation.

Enlightened by the success of the prostate robot [2], we are developing an US-guided robot to achieve quantitatively targeted liver tumor biopsy and ablation, which requires accurate registration of pre-operative 3D CT or MR liver models to 2D intra-operative US images. However, the registration is challenging due to the movement and deformation of the liver soft tissue mainly caused by the respiration [3]. At present, there are two classes of motion compensation approaches: real-time motion tracking for specific targets and model-based motion prediction.

For target-specific motion tracking, 3D US is a possible solution [4], but its small field of view limits its capacity to capture the whole organs, or track great motions possibly beyond the view, and its low voxel resolution may cause missing of small targets. Another potential scheme is to utilize a 2D US probe to track the target's in-plane motion, and move the probe swiftly to acquire additional images to derive the out-of-plane motion [5]. The limitation of this method is that only a very thin slice near the plane is scanned, and the vibration of the probe can also reduce the imaging quality and lead to inaccurate out-of-plane motion estimation.

Therefore, at present, more attention is focused on the model-based approach for motion correction [6]. With this approach, a 4D whole-liver motion model [7–12] or target-specific motion model [13–15] is first created from a sequence of MR/CT scans covering one or multiple breathing cycles at the pre-operative stage, and then applied to predict the future motion during the intra-operative stage. However, for both stages, a set of external or internal landmarks are always tracked as the surrogate respiratory signal to either form the correlation with the true motion we want to estimate, or be used as input to drive the motion model for motion compensation. On the one hand, the external landmarks, applied on the abdomen or chest, are usually tracked using special optical or electromagnetic (EM) devices [13,14]. These devices, however, create certain restrictions for surgical robots. For example, there should be no optical or magnetic obstructs along the optical or electromagnetic line of sight of these trackers. On the other hand, as internal landmarks, implanted fiducials [12] have the issue of invasiveness, leading to some infections or other complications. The inferior–superior (IS) motion of the diaphragm is also a good indicator of the breathing signal [8,9,11], but the diaphragm, as the interface between the upper abdomen and the lower lung, does not always appear in the intra-operative US liver images. Therefore, besides a real-time US imaging device to provide the view of the liver to physicians, an extra MR/US imaging device/process is required to stare at the diaphragm to provide the respiratory signal to the motion model. To overcome these problems, and particularly, to further reduce the cost of our surgical robot, and make it noninvasive, simple, and portable, we wish to identify the respiratory signals directly from intra-operative US liver images.

Since the liver motion is mainly caused by the respiration [3], the translational motion of the liver regions near the liver boundaries or vessels can well represent the respirator signal, comparable to the respiratory signal from other internal or external landmarks. In this paper, we first present an efficient and robust method for extracting the respiratory motion from intra-operative US liver images and then evaluate the consistency between the identified respiratory motion and the motion of the skin landmark recorded by an EM tracker.

Methods

The main framework of our method is shown in Fig. 1, which consists of six consecutive steps: image acquisition, video

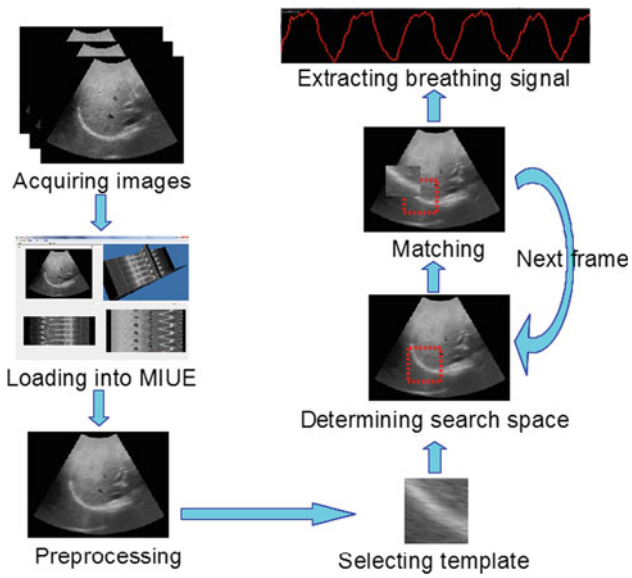

Fig. 1 The main flowchart of our method for extracting the respiratory motion signals. It can be divided into six successive stages: acquiring image sequences, loading an image sequence into MIUE, preprocessing the image sequence, selecting a specific region as the matching template, searching the optimal match frame by frame, and extracting the breathing signal

loading, pre-filtering, template region selection, frame-by-frame optimal matching, and final breathing signal extraction. After acquired using a 2D US probe to scan volunteers, the US image video is loaded into our interactive model-based image understanding environment (MIUE) platform[1] for further processing. Before extracting the breathing signal, the image sequence is preprocessed by a median filter to smooth the speckles present in the images. A template image region is then manually selected from the reference image of the dynamic image sequence. Using this template region, a frame-by-frame matching process, based on normalized cross-correlation, is executed, and the search space of each frame is determined by the matched results of the former frame. Finally, the respiratory signal of the specified region can be extracted.

Noise removal

For US images, speckle-like noises often disturb the frame-by-frame matching process and lead to unstable matching results. Therefore, a median filter is firstly employed to preprocess the image sequence before extracting the breathing pattern. This preprocess is able to remove the prominent speckle-like noises and improve the robustness and accuracy of the following matching process, which will be demonstrated in the experiments in the next section.

Template region

The selection criterion of the template image region is that this region should contain salient intensity characteristic for robust matching, such as liver boundaries or vessels, because their translational motion is highly relevant to the respiration. In addition, the size of the template image region will be carefully chosen and tuned to achieve the trade-off between the computation cost and stability of the similarity measurement. If its size is too small, it will make the matching process unstable. On the other hand, if too large, it will lose the locality of the motion, and greatly increase the time cost of the matching calculation. The experiments will show that a medium region of 65×65 pixels is appropriate for robust and fast matching.

Similarity metric

A good image similarity widely investigated and applied in image registration is mutual information (MI) [16]. However, this metric involves costly computations due to the calculation of the entropies and is more suitable for the multi-modality image registration. On the other hand, the dynamic liver US images can be respected as single-modality because the intensity may not change greatly for the successive images even though there is the respiratory motion. Hence, for this case, the normalized cross-correlation method [17] is a better choice as the image similarity metric of the registration. This metric calculates pixelwise cross-correlation and divides it by the square root of the autocorrelation of the images:

$$LC\,(A,\,B) = -\frac{1}{N}\frac{\sum_{i=1}^{N} A_i B_i}{\sqrt{\left(\sum_{i=1}^{N} A_i^2\right)\left(\sum_{i=1}^{N} B_i^2\right)}}$$

where A and B are the measured image or image region pair, and N is the number of pixels of an image or its sub-region.

Adaptive search

In image registration, the search space, including its center and size, defines the matching range of the template image on the targeted image. To achieve efficient and robust match, a basic search strategy is to determine the search space as small as possible on the targeted image. The allowable maximal search space can be the same as the searched image (640×480 pixels for the US images in this paper), but the match process is very time-consuming. For most cases, the search space can be restricted as a smaller region than the entire searched image.

Due to the quasi-periodicity of the normal respiration, the liver tissue also moves in an approximately periodical way. Therefore, the liver tissue repeatedly appears in a relatively fixed extent (1–12 mm [7]) in a normal or even deep breathing cycle, and the search space can be restricted as a neighborhood range of the template region. For instance, the experiments show that a region of 129×129 pixels is enough to find the optimal match. During the frame-by-frame matching process, the traditional search strategy is to fix the search center as the center of the template region and find the optimum near the search center, which is called as *center-fixed search strategy*. However, the experiments show that this search strategy is still very time-consuming; nearly 6 min is required for an image sequence consisting of 256 frames.

Motivated by this problem, we present a new *adaptive search strategy*, which defines a serial of small center-variant search spaces along the frame-by-frame matching process. Our search strategy makes full use of the inter-frame dependency of the US image sequence, which assumes that the motion extent of the liver tissue is small for two successive frames. Therefore, any specified image region on the former frame should appear in the small neighbor region of the same position on current frame. The optimal matching position of the former frame can be used as the center of the search space of the current frame. Based on this principle, a serial of relatively small search spaces, whose centers are automat-

[1] http://www.liversuite.com/.

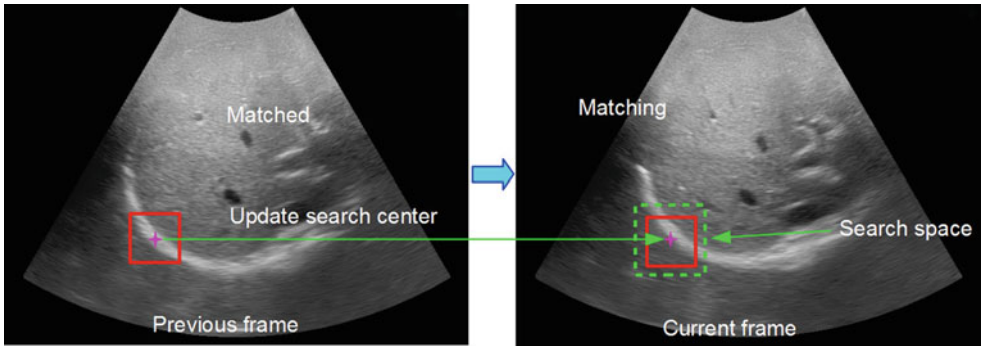

Fig. 2 The adaptive search strategy updates the search center on the current frame, according to the matched result of the previous frame. Due to the slow variation in the liver tissue on two successive frames, the search space (*dashed green square* on the *right subfigure*) can be very small

ically determined according to the former matched result, are formed along the image sequence. Here, we call center-variant search space as *adaptive search space*, and the basic matching process using adaptive search strategy is delineated in Fig. 2. Using the adaptive search strategy, we may fast and robustly extract the respiration pattern of the specified liver region.

Respiratory signal

In respiratory motion modeling, the surrogate respiratory signal is applied to firstly establish the correspondence with true motion of the liver, and then as input to the motion model for prediction or compensation. In general, the respiratory signal is certain physical measurement closely reflecting the human respiration pattern and, more importantly, should be highly relevant to the respiration-induced motion we want to estimate. For previous work on the liver motion modeling, researchers usually utilized special tracking devices to extract the respiratory signals from skin markers [13,14], implanted fiducials [12], or diaphragm [8,9,11]. In this paper, the respiratory signal is defined as 1D quasi-periodical signal extracted from the intra-operative liver US images by using our approaches.

For signal extraction, the reference image and template region are firstly specified in an interactive way; our extraction method is then applied to obtain the respiratory signal from a sequence of frame images. In essence, our matching process for each frame is a 2D rigid registration with only considering translations, which is highly related to the breathing pattern. This process searches the current frame for a corresponding region, which best matches the manually specified template region, and the 2D displacement between the matched region and the template region is recorded. After the adaptive search process is iteratively performed, a sequence of 2D displacements will be obtained. The 2D displacements reflect 2D in-plane respiratory motion of the selected liver region. We will choose the 1D direction with larger average amplitude as the surrogate respiratory signal.

The use of the surrogate respiratory signal depends on different considerations during establishing and applying these motion models [6], and its different signal attributes can all be utilized for motion model parameterization, such as the periodicity, amplitude, phase, or combination of them.

Results

Experiment setup

Figure 3 shows the experiment setup used to obtain data for the following analysis and validation. The US imaging device used is a Terason t3000 US system with a 5C2 curve linear transducer, where its US frequency is 3.5 MHz. The 2D B-mode US image sequences (with image resolution of 640×480 pixels, pixel size of about 0.37×0.37 mm and temporal resolution of 10 FPS) were obtained from four healthy volunteers with different breathing frequency, and each sequence contains 256 frames. All the experiments on extracting the respiratory motion in this paper were executed on a Dell workstation with Intel Xeon CPU E5620 2.4 GHz and 12 G RAM, and the single-thread programming mode was used. For avoiding the tremor of the probe by hands, we design a robotic arm to stably hold this US probe to acquire US images only containing the internal liver motion.

In order to validate the respiratory signals identified by our method, a NDI Aurora EM tracking system is used to track an EM sensor placed on the umbilicus of the volunteers while acquiring the US images. The anterior–posterior (AP) motion of the abdominal umbilicus is selected as reference respiratory motion for verification because the abdominal surface is usually a good position to place external marker to monitor the respiration, which is often adopted in respiratory motion modeling to obtain the surrogate breathing signals [6]. By using dynamic libraries provided by NDI and Terason vendors, we implemented a module in our software platform to record the EM signals and US images for ensuring relatively precise synchronization, each US frame correspond-

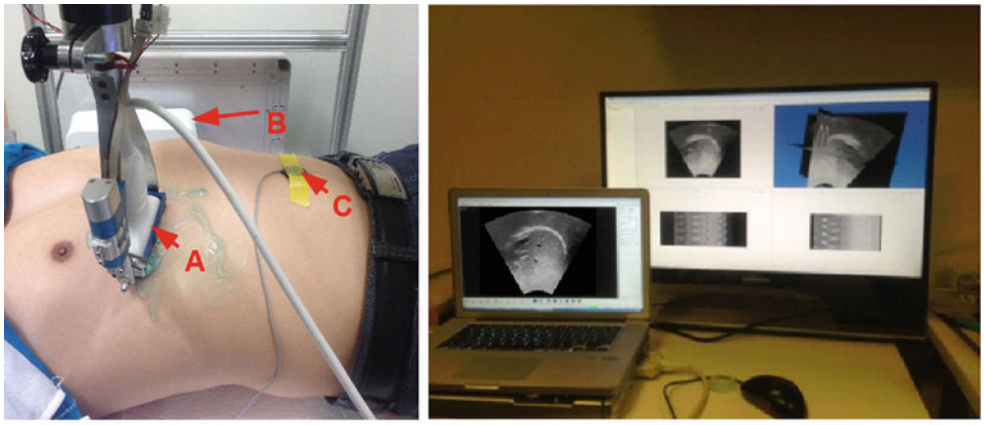

(a) US and EM tracking setup (b) Visualization for US images

Fig. 3 Setup for acquiring US images in synchronization with EM signals. In the *left photograph*, *A* on the right chest is the US transducer for imaging the right liver lobe, *B* on the left of the volunteer is a NDI Aurora EM tracking device, and *C* on the umbilicus is an EM sensor tracked by this EM device. In the *right photograph*, the laptop belongs to a part of the Terason US system, used for displaying the acquired images, which are simultaneously loaded into our MIUE framework on the bigger monitor

ing to an EM position. For each pair of EM–US data, we firstly record the EM signal and then the US image. Since the function to read the EM data executes extremely fast (more than 1000 Hz), the latency between each EM signal and US data is negligible. In addition, the US images are transferred to the computer for data processing via a fiber-optic cable, with the transmission latency of less than 3 ms ($640 \times 480 \times 8/10^9 = 2.3$ ms).

Experimental results

In this section, multiple sets of experiments were performed to analyze different aspects of our method, including effect of the noise removal, trade-off of the template region size, and efficiency and robustness of the adaptive search strategy. Finally, a set of experiments for consistency validation were executed to visually and quantitatively compare the extracted respiratory motion to the reference motion of the abdominal umbilicus tracked by the EM system.

Noise removal. In this experiment, four image sequences from four different volunteers were used, the template region was fixed to 65×65 pixels, the adaptive search space 17×17 pixels, and the filter size is gradually increased to analyze the impact of the pre-filtering on the identified respiratory motion curves. The first row in Fig. 4 displays four reference images, corresponding to the first image of each image sequence, respectively. For each reference image, an exemplary region is selected as the matching template, labelled by a red box. The second row in Fig. 4 shows four reference respiratory signals of the umbilicus tracked by the EM system while acquiring these image sequences. The last three rows list the extracted respiratory motion curves from these image sequences without filtering or with a median filter of 5×5 or 9×9 pixels. These experimental results show the median filter can eliminate the speckle-like noises present in the US images and make the frame-by-frame matching process more robust and accurate. Consequently, noises are removed from the respiratory motion curves, but the entire profile of the motion curve is well preserved.

Template region. In order to demonstrate the effect of the template region size on the resulting respiratory motion curves, a series of experiments were performed by gradually increasing the size of the template region, which is displayed in Fig. 5. For separately investigating the template region, the pre-filtering was not used and the size of the adaptive search space was fixed as 17×17 pixels. Four exemplary template regions (A, B, C, and D) from four volunteers' sequences, respectively, were selected for analysis (the first row of Fig. 5), and their sizes vary from 33×33 pixels to 129×129 pixels. It is observed that, using a template region of 33×33 pixels, the resulting motion curves are extremely unstable with heavy noises and shape distortion (the third row of Fig. 5), compared to the EM reference motion curves (the second row of Fig. 5). When the template regions grow to 65×65, 97×97, and 129×129 pixels, these motion curves basically have relatively small noises and similar shapes with the reference curves (the last three rows of Fig. 5). The matching time for different template region sizes is listed in Table 1 and linearly increases with the pixel number of the template region (the region size). For trade-off between the stableness and computation time, a square template region of 65×65 pixels can basically meet our need in spite of some noises, which can be improved by pre-filtering. Therefore, in the other experiments of this paper, the sizes of the template regions will be fixed to 65×65 pixels.

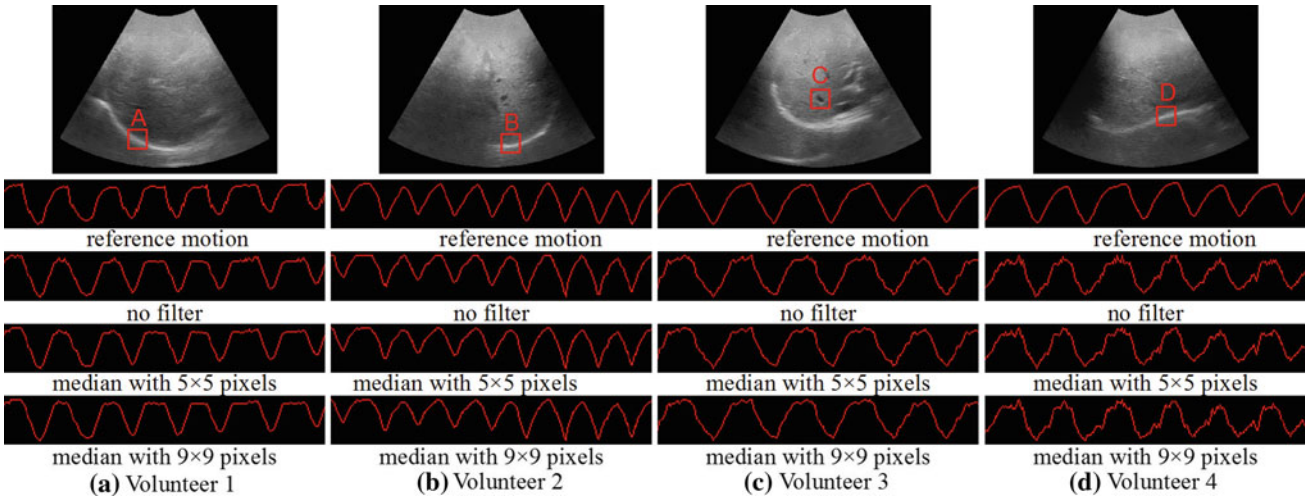

Fig. 4 Pre-filtering can improve the matching results and make the respiratory motion curves smoother. The *first row* corresponds to four reference images from the first images of four image sequences, respectively, the *second row* corresponds to the reference respiratory signals on the umbilicus tracked by the EM system, and the *last three rows* correspond to the extracted motion curves using different filtering settings

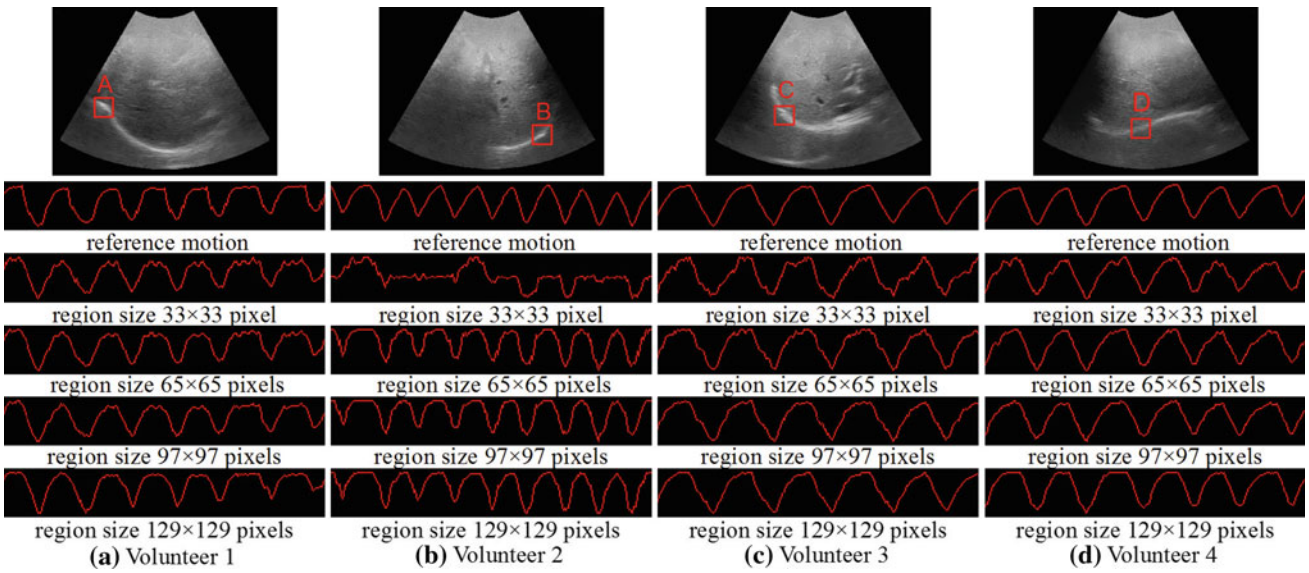

Fig. 5 Increasing the template region sizes can improve the accuracy of the extracted respiratory motion curves. The *first row* displays four reference images from four volunteers' image sequences, respectively, the *second row* lists the reference breathing patterns of the umbilicus tracked by the EM system, and the *last four rows* correspond to the extracted respiratory motion curves by increasing the template region sizes

Table 1 The search time linearly increases with the pixel number of the template region (region size)

The image sequences and corresponding template regions are the same as in Fig. 5

Template region	Region size (search time, in seconds)			
	33 × 33	65 × 65	97 × 97	129 × 129
A	1.33	5.17	11.50	20.37
B	1.33	5.15	11.53	20.26
C	1.32	5.10	11.41	20.05
D	1.33	5.24	11.63	20.38

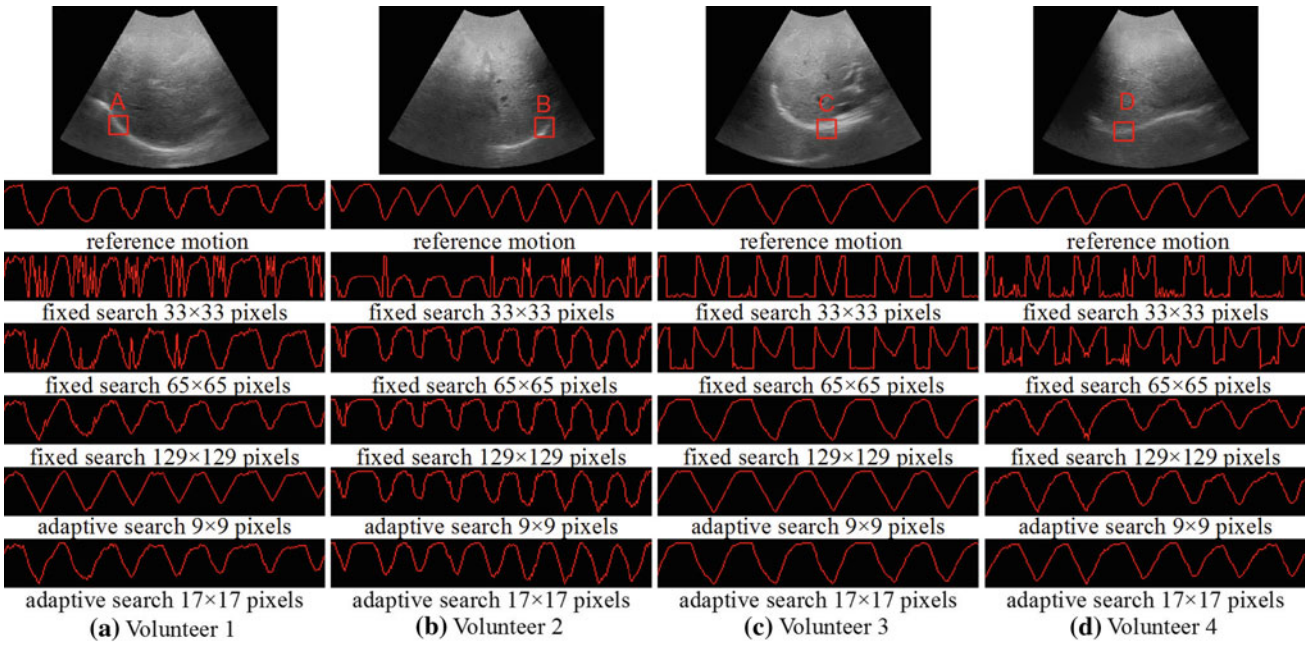

Fig. 6 Using center-fixed searching strategy, a medium search range (129 × 129 pixels) can extract good motion curves. However, using adaptive searching strategy, a relatively small search range (17 × 17 pixels) is enough

Table 2 Comparison of computation time for different search strategies

Template region	Traditional (time, in seconds)			Adaptive (time, in seconds)	
	33 × 33	65 × 65	129 × 129	9 × 9	17 × 17
A	19.31	75.10	293.34	1.43	5.08
B	19.85	76.90	304.27	1.49	5.27
C	19.46	75.26	296.17	1.44	5.13
D	19.40	75.13	295.66	1.42	5.16

The search time linearly increases with the size of the search space, and the adaptive search strategy (129 × 129 pixels) can gain a speedup of tens of times over the traditional search strategy (17 × 17 pixels) when the similar respiratory motion curves are extracted (Fig. 6). The image sequences and corresponding template regions are the same as in Fig. 6

Adaptive search. A series of experiments were performed to demonstrate the efficiency and robustness of our adaptive strategy in contrast to the traditional center-fixed search strategy. In order to focus on the search strategy, the pre-filtering was not used and the size of the template region was fixed as 65 × 65 pixels. Four typical template regions were manually selected from four volunteers' image sequences, respectively (the first row of Fig. 6, marked in red boxes), and the reference respiratory signals of the umbilicus were recorded by the EM device when acquiring each image sequence (the second row of Fig. 6). Based on the center-fixed search strategy, we cannot obtain correct respiratory motion curves using the search range of 33 × 33 or 65 × 65 pixels (the third and fourth rows of Fig. 6). Only when the search range is increased to 129 × 129 pixels (the fifth row of Fig. 6), correct respiratory motion curves are available, but leads to large computation cost. In contrast, using the adaptive search technique can find optimal match in a relatively small search range, usually a region of 17 × 17 pixels (the seventh row of Fig. 6). The computation time for the extracted respiratory motion curves in Fig. 6 is listed in Table 2. In order to obtain satisfactory respiratory curves, using adaptive searching strategy (17 × 17 pixels) can extract the curves in about 5 s for an image sequence of 256 frames in Fig. 6, while using center-invariant search technique (129 × 129 pixels) needs about 300 s. Therefore, a great speedup of the order of tens can be achieved using our proposed search technique. In addition, adaptive search strategy leads to a relatively small search range, makes the matching process more robust, and consequently alleviates the noises present in the final motion curves, which is observed by comparing the fifth and seventh rows of Fig. 6.

Consistency validation. In order to evaluate the accuracy of our method, three exemplary regions on each reference

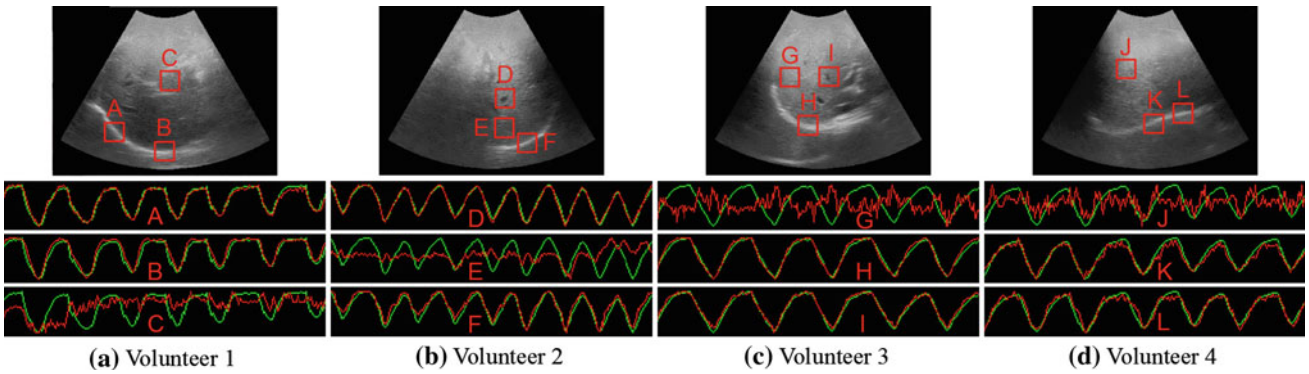

Fig. 7 Consistency is visually compared between the identified motion curves (*in red*) and the EM-tracked reference motion of the umbilicus (*in green*). The motion curves extracted near the liver boundaries and vessels highly approximate to the reference respiratory curves

Table 3 Consistency is quantitatively analyzed using the correlation coefficient (CC) metric

	Volunteer 1			Volunteer 2			Volunteer 3			Volunteer 4		
Region	A	B	C	D	E	F	G	H	I	J	K	L
Consistency	0.9591	0.9415	0.1187	0.9701	0.0627	0.9379	0.1824	0.9714	0.9798	0.1715	0.9389	0.9107

The image sequences and selected template regions are the same as Fig. 7

image of each volunteer's image sequence (the first row of Fig. 7) are selected as matching templates, and the identified motion curves (the second to fourth rows of Fig. 7, in red) are visually compared to the reference motion on the umbilicus (in green). For better visual inspection, the identified curves have been linearly scaled to have the same minimum and maximum as the EM reference curves. In addition, the indentified motion curves are also quantitatively compared with the reference motion curve using correlation coefficient (CC), which is listed in Table 3. Observed from Fig. 7 and Table 3, the motion curves extracted from the liver boundaries and vessels have nearly consistent respiratory phases with the reference curves, and the corresponding CC values are all greater than 0.9. These results show that the translational motions of the liver boundaries and vessels are highly relevant to the respiration, which reveals the potential to extract the surrogate breathing signals from intra-operative US images instead of tracking external landmarks. For other regions without the liver boundaries or vessels, the intensity values are approximately homogeneous and the contrast is very low, and thus, the translational motion is small or difficult to detect. Therefore, the identified curves near these regions are heavily inconsistent with the reference curves, and the corresponding CC values are very small, less than 0.2. All the experiments above demonstrate that some areas of the liver images carry more respiration-relevant information, such as the liver boundary and vessels, than others, and we can extract from intra-operative US liver images the surrogate respiratory signals, which is comparable to that by tracking the external landmarks. This observation supports our assumption of removing extra tracking devices from our ongoing surgical robots, which is expected to be simple, portable, and low cost.

Conclusion

A fast and robust method has been proposed to identify the respiratory motion of the liver based on its US image sequence. Using the adaptive search strategy, the method is able to achieve fast motion estimation within several seconds. The experiments also demonstrate that our method can produce accurate and robust results comparable to those of the EM tracking system. This will be of great help for the US-guided surgical robot to have a built-in respiratory motion tracking system, resulting in more compact and flexible design at relatively low cost. In future, we plan to perform more detailed validation on more subjects of different normal or abnormal breathing patterns and further demonstrate high relevance of special parts (such as the liver boundary and vessels) with the respiration. We also attempt to propose a robust method to automatically identify these special parts from intra-operative US images and finally extract their respiratory signal as the surrogate.

Conflict of interest None.

References

1. Beasley RA (2012) Medical robots: current systems and research directions. J Robot 2012:1–14

2. Ho H, Yuen JSP, Cheng CWS (2011) Robotic prostate biopsy and its relevance to focal therapy of prostate cancer. Nat Rev Urol 8:579–585
3. von Siebenthal M (2008) Analysis and modelling of respiratory liver motion using 4DMRI. Dissertation, ETH Zurich
4. Bruder R, Ernst F, Schlaefer A, Schweikard A (2011) A framework for real-time target tracking in radiosurgery using three-dimensional ultrasound. In: CARS 2011, pp S306–S307
5. Nadeau C, Krupa A, Gangloff J (2011) Automatic tracking of an organ section with an ultrasound probe: compensation of respiratory motion. In: Fichtinger G, Martel A, Peters T (eds) MICCAI 2011. Springer, Berlin, pp 57–64
6. McClelland JR, Hawkes DJ, Schaeffter T, King AP (2013) Respiratory motion models: a review. Med Image Anal 17:19–42
7. Rohlfing T, Maurer CR, O'Dell WG, Zhong J (2004) Modeling liver motion and deformation during the respiratory cycle using intensity-based nonrigid registration of gated MR images. Medical Phys 31:427–432
8. Rijkhorst E-J, Heanes D, Odille F, Hawkes D, Barratt D (2010) Simulating dynamic ultrasound using MR-derived motion models to assess respiratory synchronisation for image-guided liver interventions. In: Navab N, Jannin P (eds) IPCAI 2010. Springer, Berlin, pp 113–123
9. Rijkhorst E-J, Rivens I, Ter Haar G, Hawkes D, Barratt D (2011) Effects of respiratory liver motion on heating for gated and model-based motion-compensated high-intensity focused ultrasound ablation. In: Fichtinger G, Martel A, Peters T (eds) MICCAI 2011. Springer, Heidelberg, pp 605–612
10. Preiswerk F, Arnold P, Fasel B, Cattin PC (2011) A Bayesian framework for estimating respiratory liver motion from sparse measurements. In: Yoshida H, Sakas G, Linguraru M (eds) MICCAI 2011. Springer, Heidelberg, pp 207–214
11. Arnold P, Preiswerk F, Fasel B, Salomir R, Scheffler K, Cattin PC (2011) 3D organ motion prediction for MR-guided high intensity focused ultrasound. In: Yoshida H, Sakas G, Linguraru M (eds) MICCAI 2011. Springer, Heidelberg, pp 623–30
12. Preiswerk F, Arnold P, Fasel B, Cattin PC (2012) Robust tumour tracking from 2D imaging using a population-based statistical motion model. In: IEEE workshop on mathematical methods in biomedical image, analysis. pp 209–214
13. Khamene A, Warzelhan J, Vogt S, Elgort D, Chefd'Hotel C, Duerk J, Lewin J, Wacker F, Sauer F (2004) Characterization of Internal Organ Motion Using Skin Marker Positions. In: Barillot C, Haynor D, Hellier P (eds) MICCAI 2004. Springer, Berlin, pp 526–533
14. Ernst F, Martens V, Schlichting S, Besirević A, Kleemann M, Koch C, Petersen D, Schweikard A (2009) Correlating chest surface motion to motion of the liver using epsilon-SVR-a porcine study. In: MICCAI 2009. Springer, Berlin, pp 356–64
15. Ernst F, Bruder R, Schlaefer A, Schweikard A (2012) Correlation between external and internal respiratory motion: a validation study. Int J Comput Assist Radiol Surg 7(3):483–492
16. Pluim JPW, Maintz JBA, Viergever MA (2003) Mutual-information-based registration of medical images: a survey. IEEE Trans Med Imaging 22:986–1004
17. Tsai D-M, Lin C-T, Chen J-F (2003) The evaluation of normalized cross correlations for defect detection. Pattern Recognit Lett 24:2525–2535